

## Evaluation of the impacts of land use/cover changes on water balance of Bilate watershed, Rift valley basin, Ethiopia

Mulatu Abayicho Sulamo<sup>a,\*</sup>, Asfaw Kebede Kassa<sup>b</sup> and Negash Tessema Roba<sup>c</sup>

<sup>a</sup> Natural Resources Management Department, Jinka College of Agriculture, Jinka University, P.O. Box 165, Jinka, Ethiopia

<sup>b</sup> Hydraulic and Water Resources Engineering Department, Haramaya Institute of Technology, Haramaya University, P.O. Box 138, Dire Dawa, Ethiopia

<sup>c</sup> Water Resources and Irrigation Engineering Department, Haramaya Institute of Technology, Haramaya University, P.O. Box 138, Dire Dawa, Ethiopia

\*Corresponding author. E-mail: jkumulat13@gmail.com

 MAS, 0000-0003-3031-0547

### ABSTRACT

Land use/cover change is one of the factors responsible for changing the water balance of the watershed by altering the magnitude of surface runoff, interflow, base flow, and evapotranspiration. This study was aimed at evaluating the impacts of land use/cover change on the water balance of Bilate watershed between 1989, 2002, and 2015. The water balance simulation model (WaSiM) was used to access the impacts of land use/cover change on water balance. The model was calibrated (1989–2003) and validated (2007–2015) using the streamflow of at Bilate Tena gauging station. The result of land-use dynamics showed land use/cover change has a significant impact on the water balance of the watershed: on runoff production, base flow, interflow, evapotranspiration, and total simulation flow. In the study watershed, the change in total simulated flow increased by 77.83%; surface runoff, interflow, and base flow increased by 80.23%, 75.69%, and 87.79% respectively; and evapotranspiration decreased by 6% throughout the study period (1989–2015). The results obtained from this study revealed that the watershed is under land/cover change that shows its impacts on hydrological processes and water balance. Thus, effective information regarding the environmental response of land use/cover change is important to hydrologists, land-use planners, watershed management, and decision-makers for sustainable water resource projects and ecosystem services. Therefore, the policy-makers, planners, and stakeholders should design strategies to ensure the sustainability of the watershed hydrology for the sake of protecting agricultural activities, and urban planning and management systems within the watershed area.

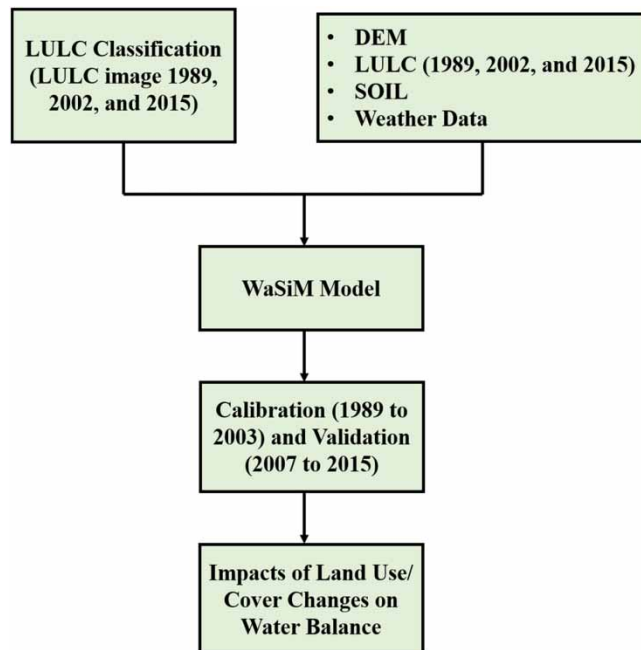
**Key words:** Bilate, land use/cover change, WaSiM model, water balance, watershed

### HIGHLIGHTS

- The research aimed to understand the LULC change impact on water balance.
- The impacts on hydrological cycle processes were determined.
- It is possible to use the WaSiM model for any watersheds.
- The model can be used for watershed managers.
- The model can be used as input for data construction of hydraulic structures.

This is an Open Access article distributed under the terms of the Creative Commons Attribution Licence (CC BY 4.0), which permits copying, adaptation and redistribution, provided the original work is properly cited (<http://creativecommons.org/licenses/by/4.0/>).

## GRAPHICAL ABSTRACT



## 1. INTRODUCTION

Long-term spatial and temporal variation of water balance components such as surface runoff, soil moisture, evapotranspiration (ET), groundwater, and streamflow can be influenced by many factors within a watershed, including land use and climate change (Deng *et al.* 2015). Land use and land cover are highly dynamic especially in developing countries that have agricultural-based economy and rapidly increasing populations.

Land cover is defined as the topography and biophysical characteristics of the earth's surface such as vegetation, water, organisms, soil, and structures created by human activities (Lambin *et al.* 2003). Land cover change has a significant influence on the quantity or quality of streamflow (Lambin *et al.* 2003). The need to manage our physical environment sustainably is caused by a growing population and the enhanced capabilities of humans to utilize the earth's resources (Farmar-Bowers *et al.* 2006).

The important part of sustainable resource use is to manage the land cover where it is, has been, or is likely to become under large stress. The human activities in utilizing and managing these land resources mainly affect the biophysical characteristics, whereas land-use change is any physical, biological, or chemical change in the conditions or the resources due to management to satisfy human interests (Farmar-Bowers *et al.* 2006).

Land-use change is one of the most visible changes in the landscapes of the world. Along with climate change, land-use change has a strong impact on the water budget and hydrology of river catchments (Defries & Eshleman 2004). One of the main challenges in recent hydrological research is assessing the effect of diverse environmental changes. Climate and land use/cover are the main factors affecting the hydrological behavior of catchments (Hörmann *et al.* 2005; Brath *et al.* 2006; Huisman *et al.* 2009).

Different studies applying different modeling approaches have identified possible land-use change impacts on catchment hydrology. Understanding the hydrological processes is crucial towards better water and land resource management; for example, hydrology, which is largely influenced by land cover and is highly important to agricultural productivity (Easton *et al.* 2010). Large changes in land use have often been associated with changes in the local hydrology, as hydrologic responses of a catchment are influenced by the land cover (Nejad Hashemi *et al.* 2011).

The major effect of land use/cover change is likely to alter the hydrologic response of sub-basins and change water availability (Mengistu 2009). The land cover under little vegetation is subjected to high surface runoff and low water retention (Tufa & Srinivasarao 2014). The land use/cover plays a fundamental role in driving hydrological processes within a sub-basin (Gwate *et al.* 2015). These include changes in water demands such as

irrigation, changes in groundwater recharge, and runoff, and changes in water quality from agricultural runoff (Guo *et al.* 2008).

Therefore, a far better understanding of land use/cover change, its effect, and interaction with the hydrology of a basin are highly essential in water supply from altered hydrological processes of infiltration, groundwater recharge, and runoff, and changes in water quality from agricultural runoff (Guo *et al.* 2008).

Ethiopia is one of the most populous countries in Africa with a population of over 94 million people (CSA 2013). Eighty-five percent of the population lives in rural areas and directly depends on the land for its livelihood (Asmamaw *et al.* 2012). This means the demand for land is increasing as the population increases. Agriculture, which depends on the availability of seasonal rainfall, is the main economy of the country. People need land for food production and housing and it is common practice to clear the forest for farming and housing activities. Therefore, the result of these activities is land use/cover changes due to daily human intervention. Hence, understanding how the land cover changes influence the hydrology of the watershed enables planners to formulate policies to minimize the undesirable effects of future land cover changes. Small-scale sub-basin-based hydrological information considering land use/cover change is crucial for hydrological processes assessment for irrigated agriculture or any use of water. Water availability is becoming a critical factor in so many sectors that the need to assess the anticipated impacts of land use/cover change on hydrology is unquestionable (Tubiello & van der Velde 2007).

Bilate watershed, which is one of the sub-watersheds of the Rift Valley basin, is facing the above types of challenges. Deforestation is a day-to-day activity for people living in and around the watershed due to increasing demand for charcoal, construction, domestic needs, expansion of arable land, and grazing areas (Degelo 2007). This continuous change in land use/cover is expected to impact the water balance of the watershed by changing the magnitude and pattern of the components of hydrological processes, which are surface runoff, baseflow, interflow, and evapotranspiration, which results in increasing the extent of the water management problem.

So, studying the impacts of land use/cover change on the water balance for Bilate watershed was crucial to solving a wide variety of water resources problems, including design of hydraulic structures; urban and highway drainage; planning of flood-control works; source pollution; disposal of waste material; evaluation of environmental impacts of land use and management practices; planning of soil conservation works and agricultural products. This enables the local governments and policymakers to formulate and implement effective and appropriate response strategies to minimize the undesirable effect of future land use/cover change (PHE; Ethiopia Consortium 2011). Similar research was done by Schulla & Jasper (2012), Kebede *et al.* (2013), Hagos (2014), and Kaiser (2014) using the WaSiM model. Therefore, this research aims to determine the land use/cover change on the water balance of the Bilate watershed using the WaSiM model.

## 2. MATERIALS AND METHODS

### 2.1. Description of the study area

Bilate River is one of the inland rivers of Ethiopia, whose source is located in the Gurage Mountains in central Ethiopia. The Bilate watershed is a part of the Main Ethiopian Rift valley basin which is part of the Great Rift Valley. The Bilate River watershed (BRW) covers an area of about 5,625 km<sup>2</sup> and is located in the Southern Ethiopian rift valley and partly in the western Ethiopian Highlands (Figure 1), and its elevation is about 1,175 meters.

### 2.2. Input data and methods

#### 2.2.1. Input data for WaSiM model

WaSiM allows various model configurations depending on the aim of the application and on the amount and quality of input data. It is possible to combine various sub-model components and to run the model in various spatial and temporal discretizations.

##### (A) Digital Elevation Model (DEM) data

Initially, 30 m by 30 m resolution DEM data was downloaded from Global Earth Explorer (USGS) <https://earthexplorer.usgs.gov> or <https://www.usgs.gov/core-science-systems/science-analytics-and-synthesis/gap/science/land-cover-data>.

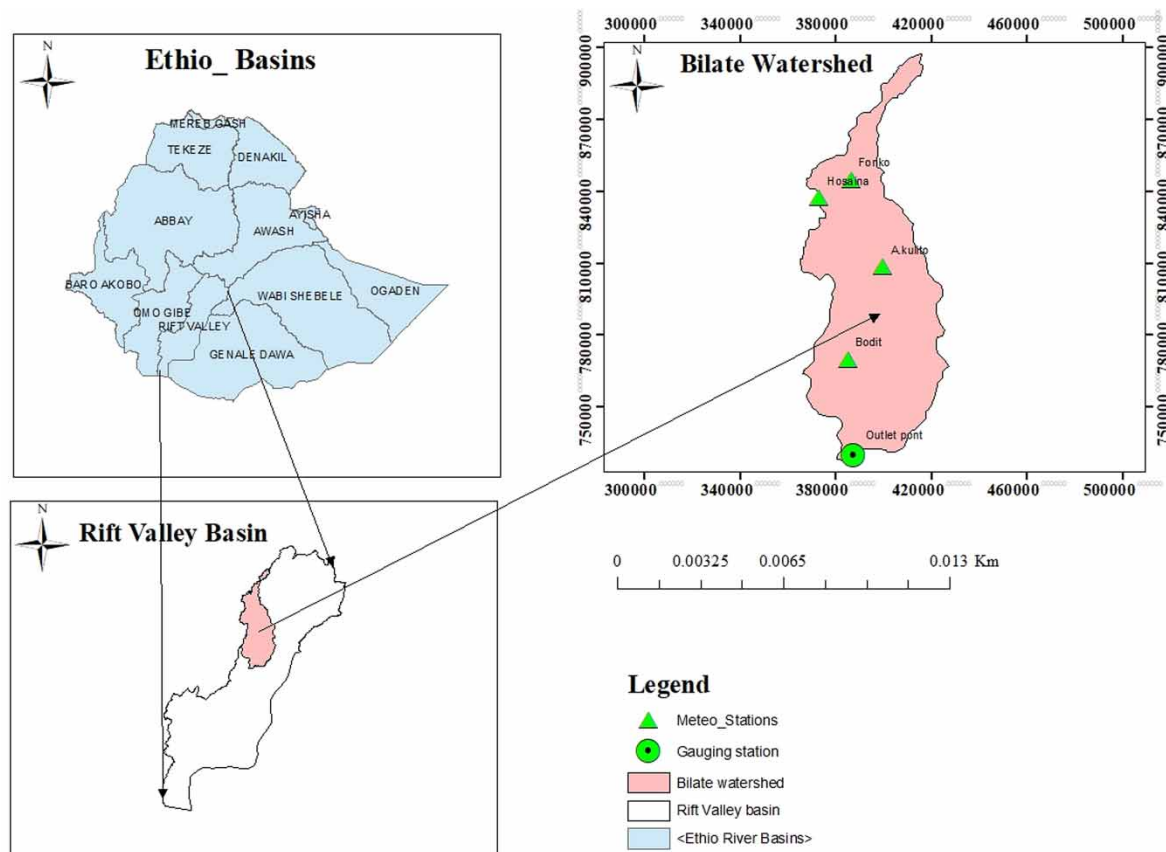


**Figure 1** | Location map of Bilate watershed.

#### (B) Soil data

The FAO/UNESCO-Soil Map of East Africa (2012), available in Arc/Info format with a scale of 1: 1,000,000, was obtained from the GIS and Remote Sensing Department, Ministry of Water, Irrigation, and Electricity of Ethiopia (MOWIE). These data were used as input for the WaSiM model.

#### (C) Land use/cover data

The land use/cover image with three years of spatial resolutions of 30 meters (1989, 2002, and 2015) (<https://www.usgs.gov/core-science-systems/science-analytics-and-synthesis/gap/science/land-cover-data>) or <https://earthexplorer.usgs.gov> were downloaded from USGS Earth Explorer and prepared using ERDAS software and ArcGIS. The WaSiM model was run for three different years' intervals of Landsat data (1989, 2002, and 2015) of land use such as Grassland/Pasture, Barren lands, Rangeland Scrublands, Cultivation/Agriculture, and Mixed Forest.

The following parameter values used as input in the WaSiM model were generated for those land uses within study period intervals: albedo, leaf area index (LAI), leaf surface resistance (Rsc), Intercept Cap, rs\_evaporation, aerodynamic roughness length (Z0), vegetation cover fraction (VCF); root depth within those different land use/cover types were obtained from different works of literature and website; <http://www.unigiessen.de/~gh1461/plapada/php/list/contentor> <http://www.unigiessen.de/~gh1461/plapada/plapada.html>.

#### (D) Meteorological data

The meteorological data required for this study were collected from the National Meteorological Agency of Ethiopia. The daily meteorological data collected for this study include precipitation, maximum and minimum temperature, relative humidity and wind speed, and sunshine hours from the years 1987–2015 in and around the watershed area for 4 stations, as shown in Table 1.

The missing meteorological daily data were filled by using the Arithmetic mean values method; hence, the total missed values were counted and compared with the data for each year, the percentage of missed data of all stations was less than 10%.

**Table 1** | Summary of selected meteorological stations

Station name	Longitude (E)	Latitude (N)	Altitude (m)	Mean annual RF (mm)	Percentage missed
A.Kulito	38° 05' 38.00"	7°18'38"	1,772	1,025	0.74
Boditi	37° 57' 18.00"	6° 57' 13.00"	2,043	1,154	1.97
Fonko	37° 58' 4.99"	7° 38' 31.99"	2,246	1,093	9.17
Hosana	37° 51' 14.00"	7° 34' 1.99"	2,307	1,100	3.74

**(E) Streamflow data**

Discharges of two gauging stations, Alaba Kulito and Tena (on Bilate River) are found in the watershed and daily flow data were collected from the Ministry of Water, Irrigation, and Electricity of Ethiopia for both gauging stations.

From the two gauging stations, the Bilate Tena gauging station was selected, because Bilate Tena gauging station was found in the same location as the outlet of the Bilate watershed. Flow data was required for performing sensitivity analysis, calibration, and validation of the model from 1989 to 2015 for the period of 27 years (Table 2).

**Table 2** | Input data for WaSiM model

No.	Description of data type	Source	Resolution	Years of data
1	DEM	Global Earth Explorer (USGS)	30 m by 30 m	1989
2	Land use/cover image	<a href="http://www.unigiessen.de/~gh1461/plapada/php/list/contentor">http://www.unigiessen.de/~gh1461/plapada/php/list/contentor</a> <a href="http://www.unigiessen.de/~gh1461/plapada/plapada.html">http://www.unigiessen.de/~gh1461/plapada/plapada.html</a>	30 m	1989, 2002 & 2015
3	Soil data	Ministry of Water, Irrigation and Electricity of Ethiopia	30 m	1992
4	Meteorological data	National Meteorological Agency of Ethiopia	–	1987–2015
5	Stream flow	Ministry of Water, Irrigation and Electricity of Ethiopia	–	1987–2015

**2.2.2. Preprocessing of data**

**2.2.2.1. Missing meteorological data estimation.** The missing data of meteorological daily data were filled by using the Arithmetic mean values method; hence, the total missed values were counted and compared with the data for each year, the percentage of missed data of all stations was less than 10%.

**2.2.2.2. Consistency test for meteorological data.** The data of the given meteorological stations was checked with the help of a double mass-curve method with reference to their neighborhood stations. It was tested using the XLSTAT 2017 Software SNHT test (Amiri 2011).

In the case of the R statistic (R stands for Range), the null and alternative hypotheses are given by  $H_0$ : the T variables are not homogeneous for what concerns their mean. Two-sided test:  $H_a$  the T variables follow one or more distributions that have the same mean. The double mass curve was used to check the consistency of the rainfall stations in the study area, and the analysis shows that the stations were consistent over the considered period.

**2.2.2.3. Filling missed hydrological data.** The daily flow data are archived based on  $m^3/s$  and transformed into mm/time step before implementation into WaSiM, since the available meteorological and hydrological data cover the same period from 1989 to 2015 used.

The missed hydrological data were filled using Regression Equation (1) with a correlation coefficient of 0.82. A regression equation was used to fill the missed hydrological data using Equation (1) from Alaba Kulito (nearby

gauging station) and with a correlation coefficient of 0.82.

$$Y = 0.5858X^{0.8077} \quad (1)$$

where

Y = dependent variables

X = explanatory/independent variables

**2.2.2.4. Areal rainfall.** Areal rainfall is the average rainfall over an area, referred to as the areal rainfall distribution and is restricted to a long-term average value. It is expressed as a mean depth (mm) over the catchment area and used to know the distribution of rainfall for the calibration and validation period (Rutebuka *et al.* 2020). Figure 2 shows the Thiessen polygon and areal proportion of each of the four selected stations in the sub-basins.

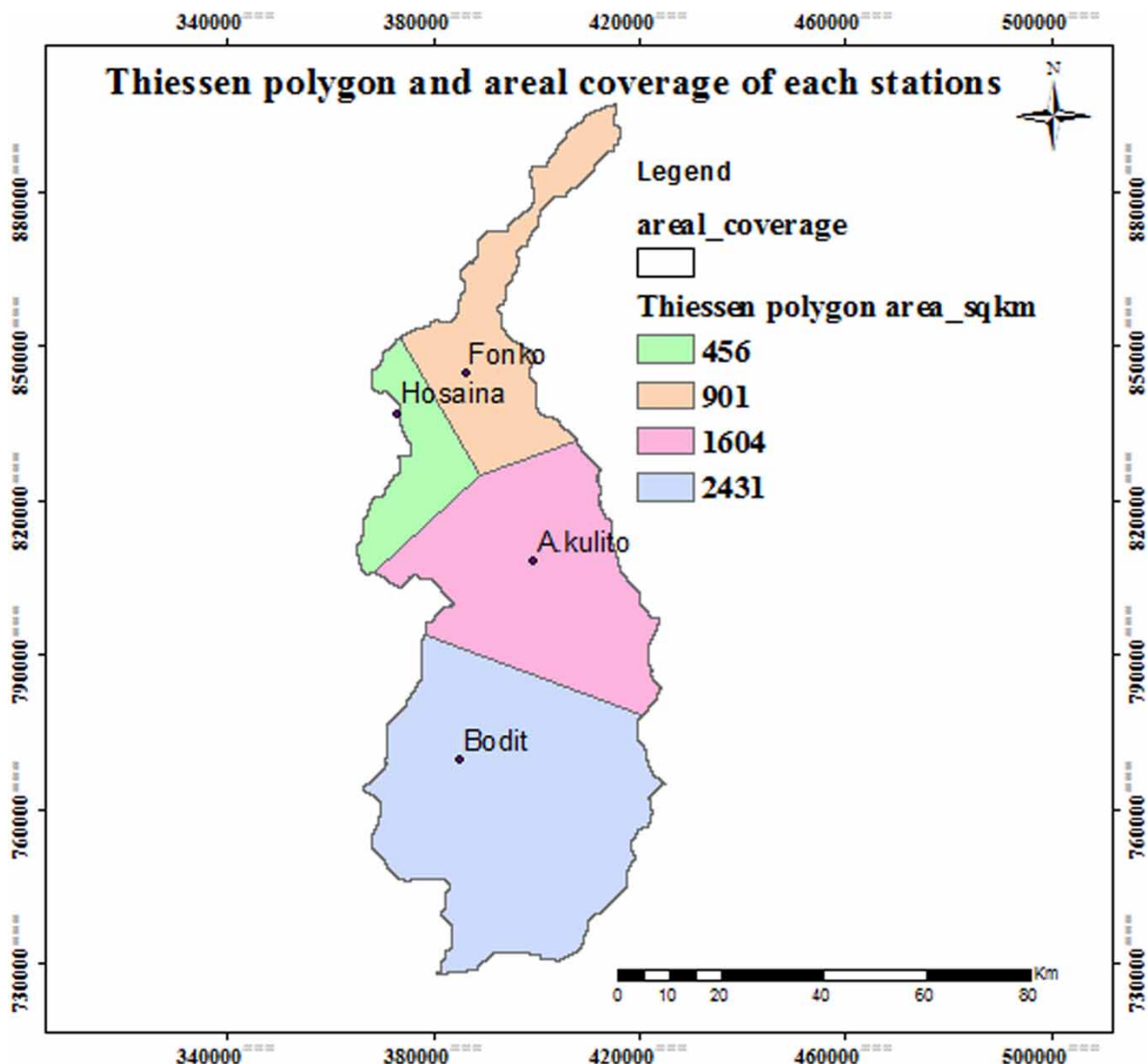


**Figure 2** | Thiessen polygon and areal coverage of each stations.

#### 2.2.2.5. Land use/cover data preparation and processing

##### (A) Landsat image processing

After delineating the watershed of the study area, land use/cover data preparation and processing is very crucial to have land cover data for the watershed. Landsat ETM<sup>+</sup> was selected for the period of 1989, 2002, and 2015 respectively. To avoid a seasonal variation in vegetation pattern and distribution throughout a year, the selection



of the acquired data was made as much as possible in the same annual season of the acquired years. The images used in this study area were orthorectified to a Universal Transverse Mercator projection using datum WGS (World Geodetic System) 84 zone 37N. The acquisition dates, sensor, path/row, resolution, and the producers of the satellite images used in this study are summarized in Table 3 below.

#### (B) Land use/cover classifications

The Land use/cover change studies were differentiated using the available data source such as remote sensing, any other relevant information, and previous local knowledge. Hence, based on the prior knowledge of the study area, ERDAS Imagine, and additional information from previous research in the study area (Degelo 2007; Wage-sho 2014; Getahun 2017), the types of land use and land cover were identified for the Bilate watershed. The descriptions of these land use and land covers are given as follows in Table 4.

All the three raster land uses of the watershed were classified into six major types (Grassland/Pasture, Range and Shrub lands, cultivation/agriculture, Mixed Forest, Settlements, and Barren land). To differentiate the cultivated land from barren lands, the season of the land use/land cover downloading was selected as December and November. To parameterize the land use in a distributed way, a land-use grid was required. The land use grid was parameterized with a land-use table that describes each grid cell with a parameter data set according to the grid classification. A specific value, which refers to a land-use type in the control-file, is assigned to each cell of this grid. The characteristics (e.g., root depth, resistance, LAI, VCF) of these types are declared in the land use table in the control-file. Most of the parameters describe a seasonal cycle with maximum (e.g., leaf area index – LAI) or

**Table 3** | Landsat images used for land use/land cover classification

Landsat image ID	Sensor type	Date acquired	Path/row	LULC year
055-1224	ETM +	Dec 24, 1989	168/55	1989
054-1130	ETM +	Dec.12, 1989	168/54	1989
054-1109	ETM +	Nov.09, 2002	168/54	2002
054-1116	ETM +	Nov.16, 2002	169/54	2002
055-1224	ETM +	Dec.24, 2015	169/55	2015
055-1217	ETM +	Dec.17, 2015	168/55	2015

**Table 4** | The major land use/land cover units and their definitions identified for the study watersheds

Major land use land cover	Their definitions
Agricultural/cultivation-lands	These include a diverse class of cultivated land, plots covered by food and commercial crops (croplands) and land units covered by residuals after immediate harvest.
Mixed-forest/Forest-lands	Forestlands usually have tree crown areal density capable of modulating the micro climate and water holding capacity of the watershed. They range from densely populated tall trees of tropical rain forest used for timber to moderately grown green forest. Forestlands could be evergreen, deciduous or mixed forestland.
Range and Shrub-lands	Range lands are typical to arid and semiarid lands characterized by xerophytic vegetation and transition zones from forest land to sparse woodlands whereas Shrub lands are a plant community characterized by vegetation dominated by shrubs, often also including grasses, herbs, and geophytes.
Grass-lands/Pasture	Grasslands are land units where the potential natural vegetation is predominantly grasses and grass-like plants. It is dominated by naturally occurring grasses as well as those areas of actual range land that have been modified to include grasses, whereas pasture land is an area covered with grass or other plants suitable for the grazing of livestock.
Water and Marshy land	Area that remains water logged and swampy throughout the year, and rivers. But water or marshy land (Boyo Lake) was not considered for this study because there is no full data to construct a lake model module in the WaSiM control file.
Barren land	Land of limited ability to support life and in which less than one-third of the area has vegetation or another cover.

minimum (e.g., stomata resistance – *rsc*) values during the vegetation period. It is easily shown that the increase of cultivation/agriculture, barren lands, and settlement area causes the decrease of mixed forest area, grasslands/pasture, and range and shrub land over the last 27 years for three LULC maps.

### (C) Accuracy assessment

The overall accuracy is used to indicate the accuracy of the whole classification (i.e. number of correctly classified pixels divided by the total number of pixels in the error matrix), whereas the other two measures indicate the accuracy of individual classes. User's accuracy is regarded as the probability that a pixel classified on the map represents that class on the ground or reference data, whereas the product's accuracy represents the probability that a pixel on reference data has been correctly classified.

In this study, the assessment was carried out using the original image for 1989 maps and the Google Earth Images for 2002 and 2015, together with previous knowledge of the area, as reference data to generate the testing data set. A total of 83, 85, and 85 testing sample points were selected randomly for the years 1989, 2002, and 2015, respectively. After completing the accuracy process as indicated in Table 6, the overall accuracy estimated as 87% is acceptable. The land cover vector data were converted into an appropriate raster format, grid size, and different land covers. The raster format of the land use map is converted to vector, to ASCII, and then to grid format, which is required as input for the WaSiM hydrological model.

**2.2.2.6. Soil data preparation.** The parameterization of the soil's physical properties is crucial for any hydrological model application. The soil hydraulic properties, which are saturated and unsaturated hydraulic conductivity and water retention, control the main hydrological processes (Fox *et al.* 2005).

The watershed was discretized into five different soil types, presented in Table 5. For the soil parameterization, the method of multiple soil horizons was used, where each soil type may have a different number of horizons. Each soil horizon has different hydraulic properties and may consist of a different number of layers of various thicknesses (Figure 3).

The parameterization of the soil physical properties for each horizon was based on the Van Genuchten parameters after Wösten *et al.* (1999) and HWSO (Harmonized World Soil Data) Viewer was used to determine percentages of silt, clay, and sand in each layer of the soil.

**2.2.2.7. WaSiM model setup.** The control file of the model was adjusted as per the watershed characteristics and available input data. Meteorological input data of the model were interpolated for each grid cell in the watershed and are followed by simulation of the main hydrological processes such as evapotranspiration, interception, infiltration, and the separation of discharge into the direct flow, interflow, base flow, and total simulated flow. These calculations are built modularly and can be adapted to the physical characteristics of the watershed. All spatial data were prepared in a raster data set (grid) with a resolution of 30 m by 30 m.

**2.2.2.8. Sensitivity analysis.** The sensitivity analysis includes test runs in which the value of only one coefficient or parameter is changed, while the values of the others remain constant. The WaSiM model sensitive parameters for this study were selected from different findings, which were made using the WaSiM model in different watersheds in Ethiopia and other basins out of our country. The sensitivity analysis was checked using the manual method by setting the values of the sensitive parameters on the WaSiM control file one after the other. From the model runs, sensitivity analysis mainly focused on the unsaturated zone model parameters, land use model (*rsc* or leaf surface resistance), and soil model (*K* recession) in the WaSiM-control file but the most sensitive parameters were found in the unsaturated zone model, as shown in Table 6.

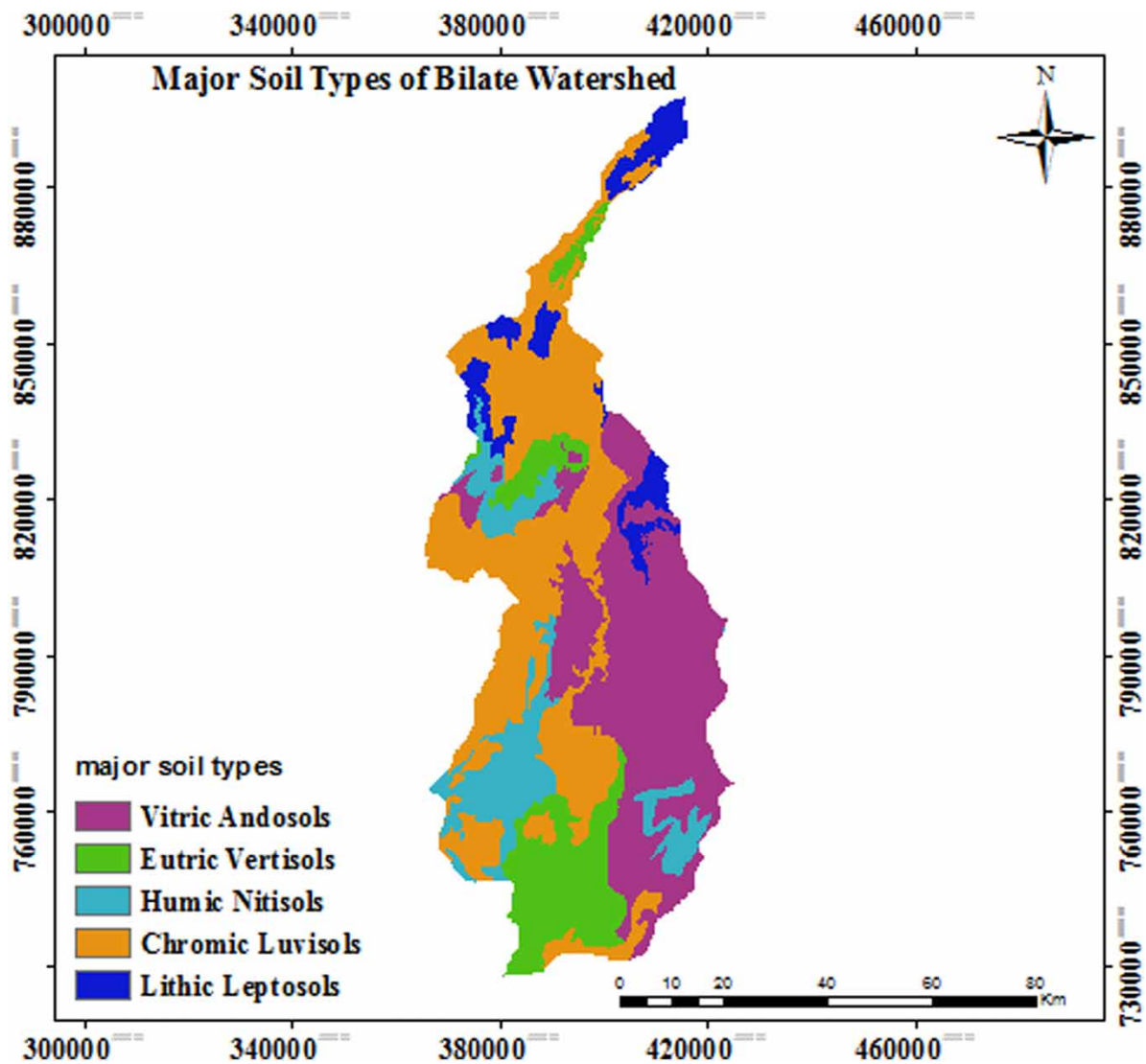
### 2.2.3. Determining the water balance of the watershed

The water budget simulation section of WaSiM comprises a chain of modules that combine both the physical and empirical descriptions of water flow. In this study, constant climatic conditions under changing land use or land cover were considered. The following components or model modules were used to calculate the water balance of watersheds.



**Table 5** | WaSiM codes for major soil map of Bilate watershed

WaSiM codes for major soil map	Definition for major soil map
1	Eutric Vertisols
2	Vitric Andosols
3	Chromic Luvisols
4	Humic Nitisols
5	Lithic Leptosols

**Figure 3** | Major soil types of Bilate watershed.**Table 6** | List of model optimal parameters

List of parameters	Description
Rsc	For land use
$k_{rec}$ (recession constant)	For the saturated hydraulic conductivities
$Q_{o_{max}}$	For base flow(when the soil is saturated)
$d_r$ (drainage density)	For interflow

2.2.3.1. *Potential and real evapotranspiration.* The model uses the Penman-Monteith formula to calculate evapotranspiration

$$\lambda E = \frac{3.6 \left( \frac{\nabla}{\gamma_p} \right) \cdot (R_N - G) + \frac{p \cdot c_p}{\gamma_p \cdot \gamma_\alpha} \cdot (e_s - e) \cdot t_i}{\frac{\nabla}{\gamma_p} + 1 + \frac{\gamma_s}{\gamma_\alpha}} \quad (2)$$

where  $\nabla$  = Latent vaporization heat [KJ·Kg<sup>-1</sup>];  $\lambda = (2500.8 - 2.372 \cdot T)$ ;  $T$  = temperature in °C;  $E$  = latent heat flux (kg·m<sup>-2</sup>);  $\Delta$  = tangent of the saturated vapor pressure curve [hPa·K<sup>-1</sup>];  $R_N$  = net radiation, conversion from Wh·m<sup>-2</sup> to KJ·m<sup>-2</sup> by factor 3.6; [wh/m<sup>-2</sup>];  $G$  = soil heat flux [wh/m<sup>-2</sup>];  $p$  = density of dry air (kg·m<sup>-3</sup>);  $c_p$  = specific heat capacity of dry air (KJ(KgK)<sup>-1</sup>) at constant pressure ;  $e_p$  = saturation vapor pressure at temperature  $T$  [hPa];  $e_a$  = actual vapour pressure (hPa)  $t_i$  = number of seconds within a time step;  $\gamma$  = psychrometric constant [hPaK<sup>-1</sup>];  $r_s$  = bulk-surface resistance [s·m<sup>-1</sup>];  $r_a$  = bulk-aerodynamic resistance [s·m<sup>-1</sup>].

2.2.3.2. *Interception.* Interception is that part of precipitation caught up by the canopy formed by the vegetation above the ground. For WaSiM, the simple bucket approach is used for the computation of interception storage, which is dependent on the total leave coverage (a factor of LAI) and the maximum height of the water layer on the vegetation.

$$SI_{\max} = V \cdot LAI \cdot h_{SI} (1 - v) \cdot h_{SI} \quad (3)$$

where  $SI_{\max}$  = maximum interception storage capacity [mm];  $v$  = degree of vegetation coverage [m<sup>2</sup>/m<sup>-2</sup>];  $LAI$  = leaf area index [m<sup>2</sup>/m<sup>-2</sup>];  $H_{SI}$  = maximum height of water [mm].

2.2.3.3. *Infiltration and the unsaturated zone module.* WaSiM uses after (Green & Ampt 1911) stems from the principle that, when saturation is reached or in situations when precipitation intensity exceeds infiltration capacities, almost all the excess precipitation is channeled into the direct runoff, and the infiltration is calculated as if  $PI > k_s$ ,

$$t_s = \frac{t_s \cdot n_a}{PI} = \frac{\frac{\psi f}{PI} - 1}{\frac{k_s}{PI}} \quad (4)$$

where  $t_s$  = saturation deficit from the beginning of the time step [h];  $L_s$  = saturation depth [mm];  $n_a$  = fillable porosity ( $n_a = \theta_s - \theta$ ) [-];  $\psi f$  = suction of the wetting front ( $a \approx 1000n$ ) [mm];  $PI$  = precipitation intensity [mm·h<sup>-1</sup>];  $K_s$  = saturated hydraulic conductivity [mm·h<sup>-1</sup>].

2.2.3.4. *Soil model.* WaSiM versions with a physically based soil model use the RICHARDS equation for modeling the fluxes within the unsaturated soil zone. The modeling is done one-dimensionally in the vertical direction using soil with several numeric layers. The continuity equation for this type of problem is given by:

$$\frac{\partial \Theta}{\partial t} = \frac{\partial q}{\partial Z} = \frac{\partial}{\partial Z} \left( -k(\Theta) \frac{\partial \psi(\Theta)}{\partial z} \right) \quad (5)$$

where  $\Theta$  water content [m<sup>3</sup>/m<sup>3</sup>];  $t$  = time [s];  $k$  = hydraulic conductivity [m/s];  $\psi$  = hydraulic head as the sum of the suction  $\psi$  and geodetic altitude  $h$  [m];  $q$  = specific flux [m/s];  $Z$  = vertical coordinates [m]; the soil model is used to calculate the vertical flow of water in the unsaturated zone.

The WaSiM uses the Richards equation for modeling the fluxes within the unsaturated soil zone and the fluxes will be calculated by the equation;

$$\frac{\Delta \Theta}{\Delta t} = \frac{\Delta q}{\Delta z} = q_{in} - q_{out} \quad (6)$$

where  $\Theta$  = water content [ $\text{m}^3/\text{m}^3$ ];  $t$  = time [s];  $q$  = specific flux [ $\text{m}/\text{s}$ ];  $z$  = vertical coordinate [m];  $q_{\text{in}}$  = inflow into the actual soil layer [ $\text{m}/\text{s}$ ] and  $q_{\text{out}}$  = the outflow from the actual soil layer (including interflow and artificial drainage) [ $\text{m}/\text{s}$ ] (Schulla & Jasper 2012).

The dependencies of the hydraulic properties on the water content of the soil are considered discretely. The flux  $q$  between two layers with indices  $u$  (upper) and  $l$  (lower) is then given by:

$$q = k_{\text{eff}} \cdot \frac{h_h(\Theta_u) - h_h(\Theta_l)}{0.5 \cdot (d_u + d_l)} \text{ with } \frac{1}{k_{\text{eff}}} = \frac{d_u}{d_{l+d_u}} \cdot \frac{1}{k(\Theta_u)} + \frac{d_l}{d_{l+d_u}} \cdot \frac{1}{k(\Theta_l)} \quad (7)$$

where  $q$  = flux between two discrete layers  $\text{m}/\text{s}$ ;  $k_{\text{eff}}$  = effective hydraulic conductivity  $\text{m}/\text{s}$ ;  $h_h$  = hydraulic head, dependent on the water content and given as difference of geodetic altitude  $h_{\text{geo}}$  [m] and suction  $\psi(\Theta)$  after equation;  $d$  = thickness of the layers under consideration [m]; the basin under this study was subdivided into hydrological sub-basins. The discharge at the outlet of each sub-basin was calculated by the sub-models mentioned above; then, the discharge at the outlet of the entire watershed area was calculated by routing the discharge of the individual sub-basins through the interconnecting rivers and channels.

$$Q_{\text{out}} = (Q_{v,i-1} \cdot e^{\frac{-\Delta t}{K_v}} + Q_{v,i}(1 - e^{\frac{-\Delta t}{K_v}})) + ((Q_{h,i-1} \cdot e^{\frac{-\Delta t}{K_h}} + Q_{h,i}(1 - e^{\frac{-\Delta t}{K_h}})) \quad (8)$$

where  $I$  = interval number;  $\Delta t$  = time step [h];  $K_v$  = storage coefficient flood plains [h];  $K_h$  = storage coefficient main channel [h];  $Q_{\text{out}}$  = outflow of the channel during the time [mm];  $Q_v$  = discharge on flood plains [mm];  $Q_h$  = discharge in the main channel [mm].

The simulated water balance components, which were generated from LULC\_1989, LULC\_2002, and LULC\_2015, of total simulated flow, interflow, base flow, potential evapotranspiration, real evapotranspiration, and infiltration were analyzed for those land use maps. Thus, the general methodology was continued by applying the three LULC map data (Landsat images) and analyzing the impacts of land use land cover change on water balance for three LULC maps. Finally, the water balance of the watershed area was determined using Equation (7) for Bilate Watershed for those land use land cover maps, and change in storage was also computed using Equation (8).

$$\Delta S = P - \text{ETR} - Q \quad (9)$$

where,  $Q$  is the runoff,  $P$  the precipitation,  $\text{ETR}$  the evapotranspiration, and  $\Delta S$  the change in soil storage. All variables were represented in mm per time step for the whole watershed area.

### 3. RESULTS AND DISCUSSION

#### 3.1. Land use/cover analysis

##### 3.1.1. Overall accuracy, producer's accuracy, and user's accuracy

The accuracy assessment is used to determine the correctness of the classified image. It was performed using a confusion matrix. The overall accuracy gives the overall results of the confusion matrix. It is calculated by dividing the total number of correct pixels (diagonals) by the total number of pixels in the confusion matrix. The overall accuracy for the maps of 1989, 2002, and 2015 were 87, 80, and 91% respectively hence, they fulfill the minimum requirements.

The producer's accuracy tells us how well a certain area can be classified. It is obtained by dividing the number of correctly classified pixels in the category by the total number of pixels of the category in the reference data. The producer's accuracy is also known as an Omission Error, which is the probability of reference pixels being classified correctly. It gives only the proportion of correctly classified pixels. The overall result of the producer's accuracy ranges from 69% to 93% as indicated in Table 7.

User's accuracy is the ratio between the total number of pixels correctly belonging to a class (diagonal elements) and the total number of pixels assigned to the same class by the classification procedure (row total). This quantity explains the probability that a pixel of the classified image truly corresponds to the class to which it has been assigned. In this study, the user's accuracy ranges from 80% to 93%.

**Table 7** | Confusion matrix of LULC classification data

		LULC classification data						Total	Users accuracy
		CL	RL	GL	MF	S	BL		
LULC classification data	CL	18		1	1			20	90
	RL	1	12			1	1	15	80
	GL	1		16		1		18	89
	MF	1	1		10			12	83
	S	1		1		15		17	88
	BL	1					14	15	93
	Total	22	13	18	11	17	15	97	
Producers accuracy(%)		82	92	89	90	88	93		Overall accuracy = 87

Note: CL, cultivation/agricultural land, RL, Range land, GL, grass land, MF, mixed forest, S, settlement, and BL, bare land.

### 3.1.2. Land use/cover maps

The land use/land cover map of 1989 in [Tables 8 and 9](#) shows that the total cultivated land/agriculture coverage class was about 28.92% of the total area of the watershed. It increased rapidly and became 34.12% and 43.3 of the watershed in 2002 and 2015 land use land cover maps respectively. This is mainly because of the population growth that caused the increase in demand for new cultivation land and settlement, which in turn resulted in shrinking of other types of land use land cover of the area. The forest coverage in 1989 was about 21.79% of the total area of the watershed. However, in the year the 2002 and 2015, this was reduced to almost 12.79% and 6.4% of the total area respectively. This is most probably because of the deforestation activities that have taken place for agriculture and the expansion of settlements.

**Table 8** | WaSiM codes for different LULC maps

WaSiM codes for three LULC data			
LU1989	LU2002	LU2015	Definition for major LULC
1	1	2	Grasslands/Pasture
2	2	5	Range and Shrub lands
3	3	4	Cultivation/agriculture
4	4	1	Mixed Forest
5	5	3	Settlements
6	6	6	Barren lands

**Table 9** | Areal coverage of reclassified land use/land cover condition for study watershed

Land use/land cover class	Percentage land use/land cover			Percentage change		
	1989	2002	2015	1989–2002	2002–2015	1989–2015
Grasslands/Pasture	10.48%	11.11%	8.08%	6.00%	-20.79%	-22.00%
Range and Shrub lands	26.35%	23.24%	15.06%	-12.00%	-35.00%	-43.00%
Cultivation/agriculture	28.92%	34.12%	43.30%	18.00%	27.00%	50.00%
Mixed Forest	21.79%	12.30%	6.40%	-43.00%	-48.00%	-71.00%
Settlements	10.25%	16.23%	21.98%	58.00%	35.00%	114.00%
Barren lands	2.20%	3.00%	5.18%	30.00%	73.00%	135.00%

The individual class areas and change statistics for the three periods are summarized in [Table 9](#). The results of previous studies showed the same fact in the Bilate watershed. For example, [Wagesho \(2014\)](#) and [Wakjira \(2016\)](#) reported that cultivation and settlements of Bilate watershed were increased by 61.6% and the mixed forest decreased to 67.7% from 1976 to 2000. Hence, the impacts of land use/cover change of the Bilate watershed are indicated in [Figures 4 and 5](#).

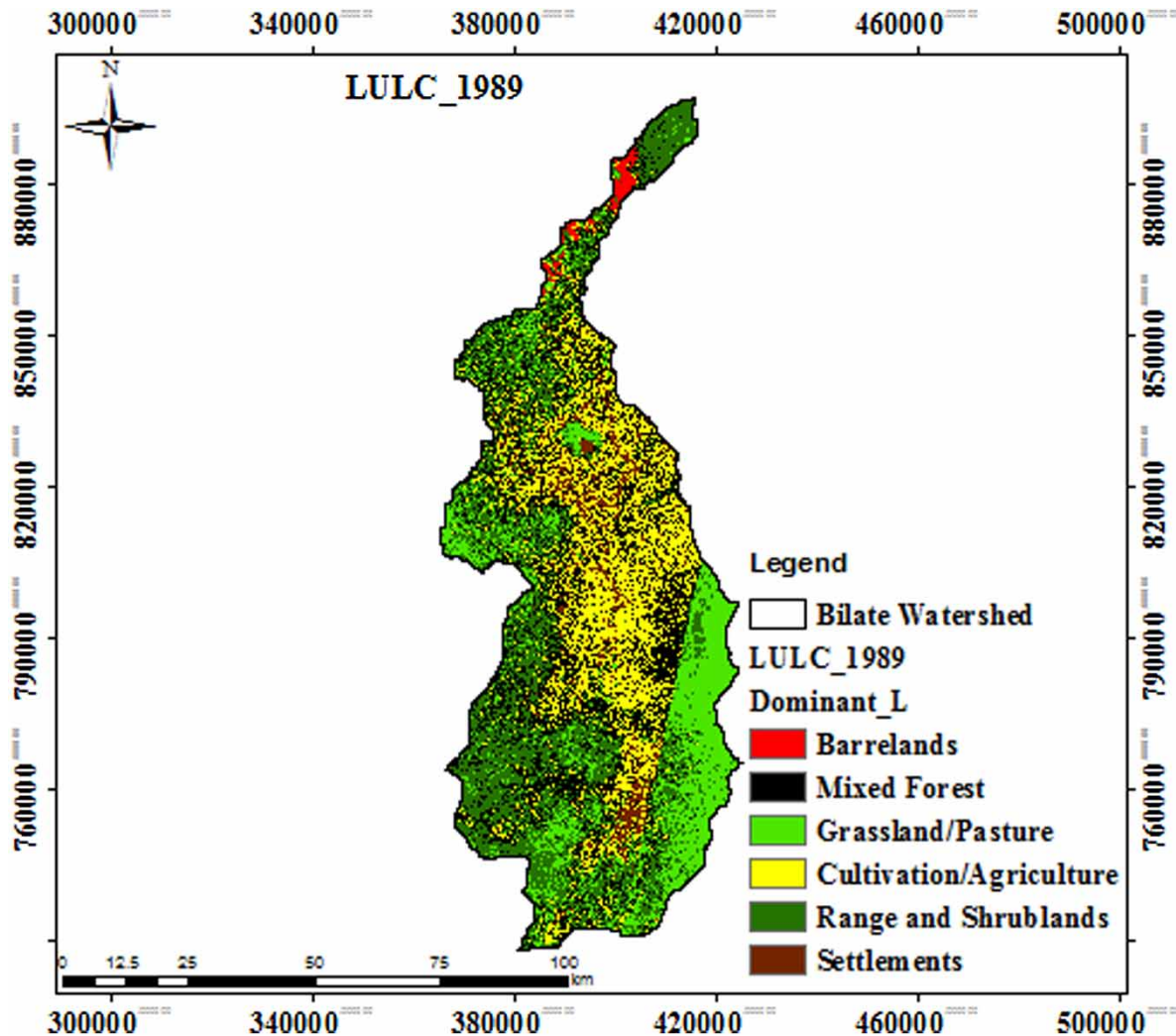


**Figure 4** | LULC\_ 1989 map of Bilate watershed.

### 3.2. Sensitivity analysis

The executed sensitivity analysis mainly focused on the unsaturated zone model parameters. Table 10 shows the results of the sensitivity analysis. Both  $Q_0$  and  $k_B$  are quite sensitive to the base flow, as expected. Furthermore,  $k_D$  is considerably sensitive to peak flow. Finally, the drainage parameter  $dr$  seems to be quite sensitive to the base flow. An increase in the  $k_B$  value always results in an increased base flow value for low flow conditions at the beginning of the calibration period. Finally, the higher the  $k_D$  value, the lower the direct flow and when the value of  $K_i$  increased, the value of the interflow becomes lower. A similar analysis was done by Kaiser (2014).

### 3.3. Model calibration and validation

The WaSiM sensitive parameters were identified/selected from other authors' findings: Schulla & Jasper (2012), Kebede *et al.* (2013), Hagos (2014), and Kaiser (2014). Finally, the sensitive parameters for this study are listed in Table 10 and the maximum, minimum, and optimum values of the sensitive parameters of this study are identified, as indicated in the table.

As reported in Kebede *et al.* (2013), the parameters such as  $rs_{\text{evaporation}}$  (soil surface resistance for evaporation only) and  $rsc$  (leaf surface resistance) were also calibrated manually. The other parameters in the soil water dynamics of the WaSiM-ETH were  $K_D$  and  $K_I$  (Table 10), which control the surface runoff and interflow storage effects in the Richards equation, which was used for this study. Finally, the parameters  $K_{rec}$ ,  $dr$ ,  $K_D$ , and  $K_I$  were found to be very sensitive. From all of these sensitive parameters,  $d_r$  was the most sensitive parameter.

As the model analysis of this research indicated, the hydrographs were good at simulating the daily, weekly, and monthly scales. The monthly simulation indicates better than daily and weekly simulation for this study.



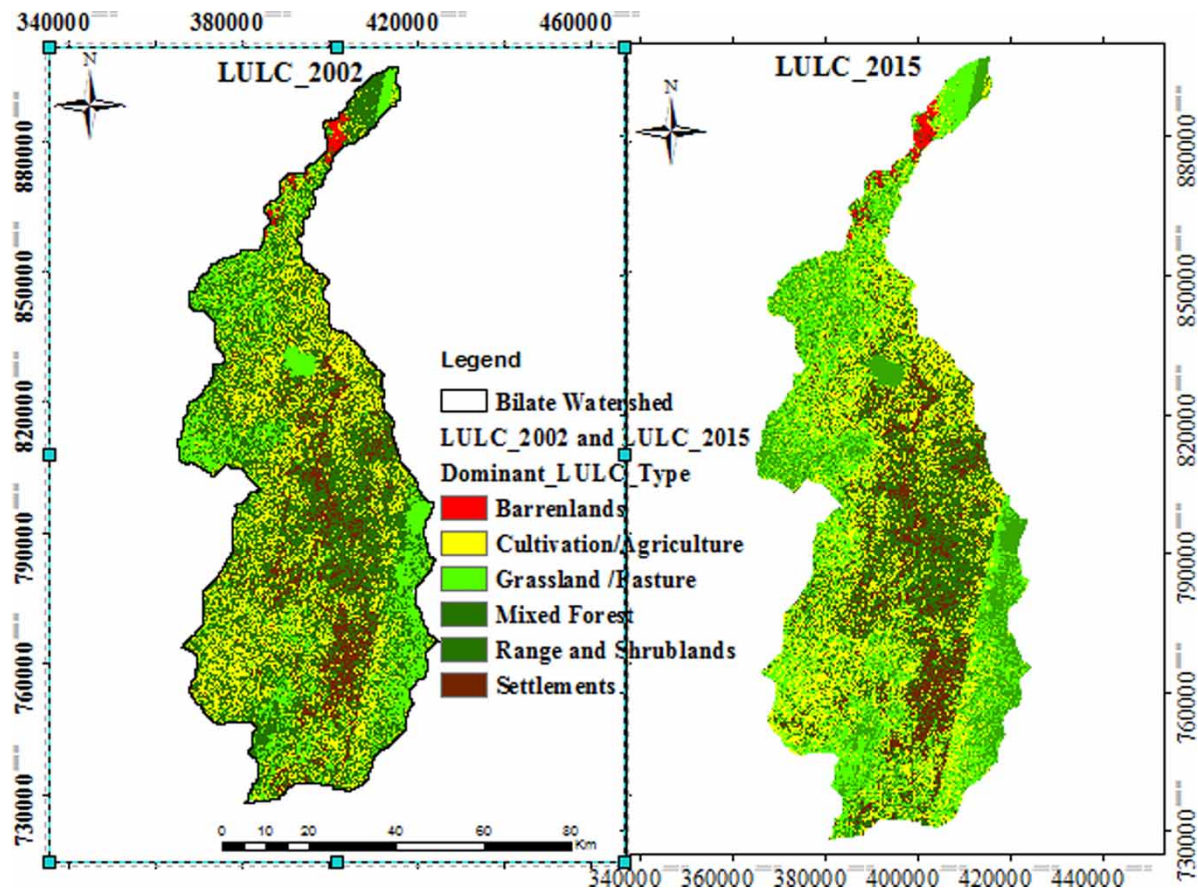


**Figure 5** | Map of LULC\_2002 and LULC\_2015 of Bilate watershed.

**Table 10** | WaSiM sensitive parameters selected for the calibration of the hydrologic processes, final values and ranges

Parameter	Description	Optimum value	Ranges	
			Min	Max
$k_D$ [h]	Recession constant for direct runoff	220	0	220
$K_I$ [h]	Recession constant for interflow	100	0	100
$d_r$ [m-1]	Drainage density	60	10	80
$K_B$ [h]	Recession constant for base flow	0.155	0	1
$K_{rec}$ [-]	Recession constant for saturated hydraulic conductivity with depth	0.9	0.1	1
rs-evaporation [s/m]	Soil surface resistance (for evaporation only)	80	20	100
rsc [s/m]	Leaf surface resistance	250	50	300

From the results indicated in Table 10, the index of agreement  $d$  lies in the range of 0.0–1.0 with higher values indicating better agreement. Similarly, NSE and EVC range from minus infinity to 1.0, with higher values indicating better agreement, and a value of 1.0 being the optimal value.

The coefficient of efficiency ( $R^2$ ) and Nash Sutcliffe model efficiency (NSE) values were used to examine model performance and the result indicates 0.85 and 0.89 to the coefficient of efficiency ( $R^2$ ) and 0.85 and 0.89 to Nash Sutcliffe model efficiency (NSE) during calibration and validation respectively, but the model shows underestimation in some years because some flow data problems show the outliers (Figures 6–9). From the other findings, Wagesho (2014) reported 0.78 ( $R^2$ ) and 0.611 (NSE) for the calibration and 0.78 ( $R^2$ ) and 0.623 (NSE) for



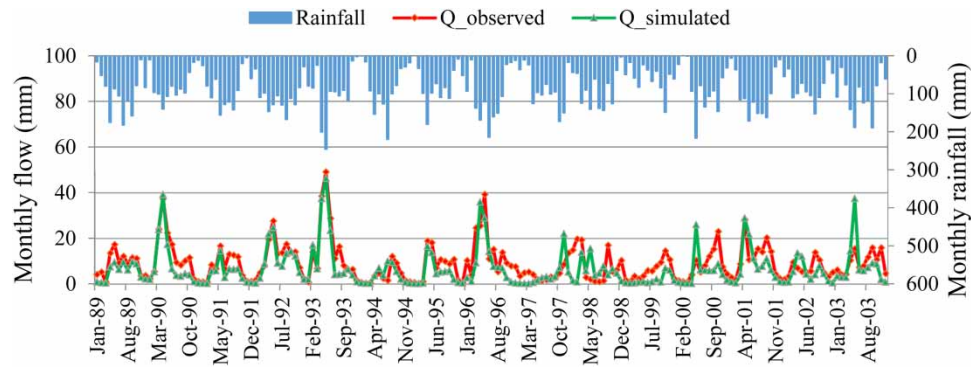


**Figure 6** | Monthly calibration results (1989–2003) using LULC\_1989 data.

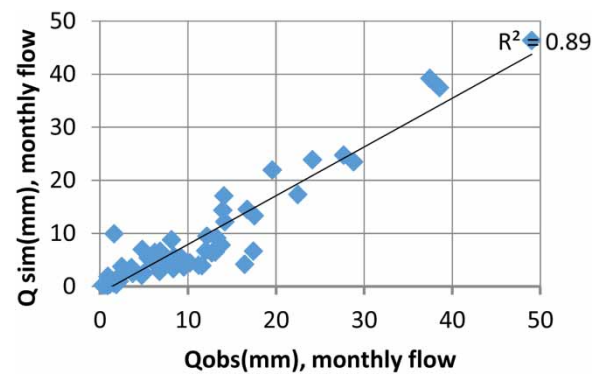


**Figure 7** | Correlation graph of monthly Qsim and Qobs for calibration period using LULC\_1989 data.

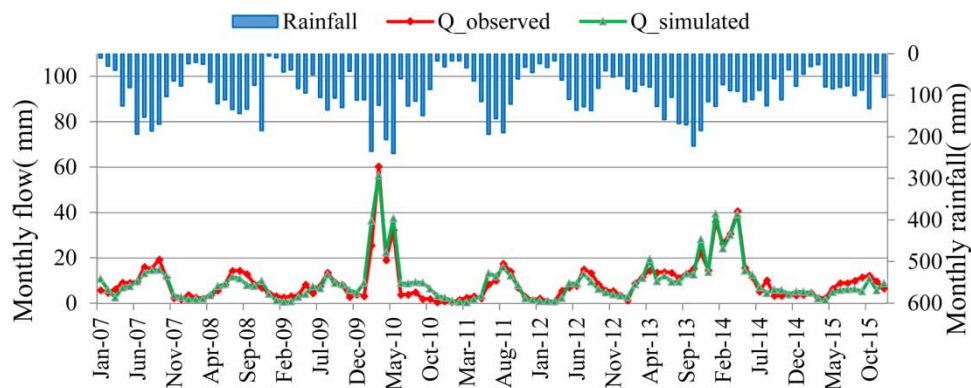


**Figure 8** | Monthly validation results (2007–2015) using LULC\_1989 data.

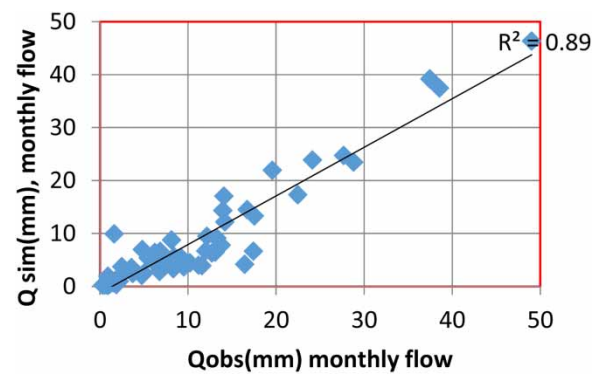


**Figure 9** | Correlation of Qsim and Qobs for validation period using LULC\_1989 data.

validation using the HEC HMS model and [Getahun \(2017\)](#) reported, 0.79 ( $R^2$ ) and 0.78 (NSE) for calibration and 0.64 ( $R^2$ ) and 0.60 (NSE) for validation using the SWAT model in Bilate watershed.

To evaluate the general model performance of the distributed hydrological model, [Brincker et al. \(2001\)](#) suggest the following graduation of the achieved model efficiency. Based on general performance criteria, the model indicated good performance since the values of  $D_V$  and  $R^2$  for the calibration and validation period were 17.42, 0.85, and 10.5, 0.89 respectively ([Table 11](#)).

**Table 11** | Summary of performance of the WaSiM model for the daily, weekly and monthly calibration and validation period between 1989–2003 and 2007–2015 respectively for Bilate watershed

Criteria	Daily		Weekly		Monthly	
	Calibration 1989–2003	Validation 2007–2015	Calibration 1989–2003	Validation 2007–2015	Calibration 1989–2003	Validation 2007–2015
$E_V$	0.77	0.82	0.87	0.70	0.89	0.93
$R^2$	0.73	0.77	0.82	0.96	0.85	0.89
RMSE	0.19	0.24	0.41	0.01	0.71	0.71
NS	0.73	0.77	0.82	0.96	0.85	0.89
Coefficient of determination	0.77	0.48	0.86	0.58	0.89	0.90
Index of agreement	0.93	0.93	0.95	0.99	0.96	0.97

### 3.4. Performance of WaSiM model for Bilate watershed

#### 3.4.1. Impacts of LULCC on water balance of Bilate watershed

The analysis of the LULCC contribution was made on surface runoff; interflow, base flow, total simulated discharge, and evapotranspiration as characteristics of the hydrological process of the watershed. The contribution of surface runoff, total simulated flow, and interflow have increased from 1989 to 2015, as indicated in [Figure 11](#). This was related to the surface cover of the watershed since changing the forest land of the watershed to agricultural land accelerated the runoff rate and reduced the infiltration of soil moisture content ([Table 8](#)). From the result of the land use land cover map, areas of forest have decreased from 1989 to 2015, which has contributed to the increasing surface runoff contribution. In the same manner, [Wagesho \(2014\)](#) reported that the simulated surface runoff component increased progressively since the 1970s in Bilate watershed. As in [Bahati et al. \(2021\)](#), the historical/current minimum, maximum, and mean annual flow of Muziz river, future minimum, maximum, and mean annual flow will increase respectively.

On the other hand, the rate of evapotranspiration has decreased from 1989 to 2015, indicating losses are mainly through evapotranspiration. These result revealed that the land use/land cover change has significant impacts on infiltration rates, on runoff production, total simulation flow, interflow, base flow, evapotranspiration, and water retention capacity of the soil or change in storage of the soil; hence, it affects the water balance of the watershed. This is because the land cover under little vegetation is subjected to high surface runoff, low water retention, and low evapotranspiration ([Tufa & Srinivasarao 2014](#)). The changes in water balance (hydrological process) under the land use/land cover changes are summarized in [Figure 10](#).

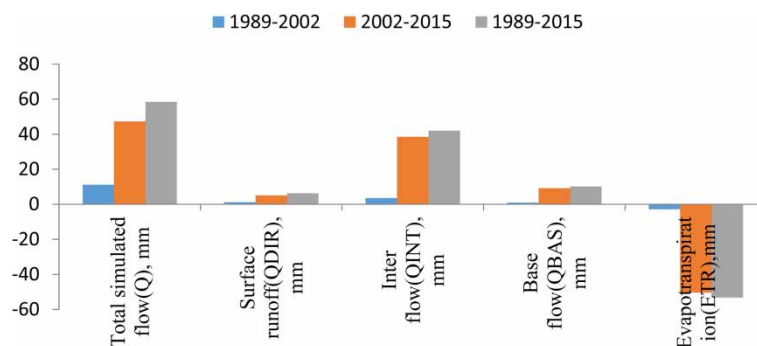


**Figure 10** | Changes of hydrological process over the period of study time intervals through three land use land cover types.

As shown in Tables 12 and 13, the simulated water balance for the Bilate watershed using the WaSiM-ETH reveals the interflow component of the water balance takes a higher fraction of simulated discharge. The change in soil water storage  $\Delta S$  is the result of the balance, being positive when the profile has a net gain of water, and negative for a net loss (Reichardt *et al.* 1995). From the results, the mean annual stream flows were evaluated due to land use/land cover change in the Bilate watershed, as shown in Figure 11.

**Table 12** | Annual water balance (in mm) for Bilate watershed area for the calibration period (1989–2003) for LULC\_1989

Year	P	ETR	Q	$\Delta S$	Q <sub>DIR</sub>	Q <sub>INT</sub>	Q <sub>BAS</sub>
1989	1041.13	940.62	64.55	35.96	5.65	44.01	14.89
1990	969.69	869.64	111.29	–11.24	10.05	91.01	10.24
1991	917.52	806.86	52.62	58.04	4.51	40.29	7.82
1992	1168.82	976.98	122.14	69.70	14.86	86.45	20.84
1993	1148.50	1015.16	156.92	–23.58	17.78	126.04	13.10
1994	964.37	834.09	43.19	87.09	3.60	29.94	9.66
1995	882.95	752.16	55.02	75.77	4.86	38.55	11.60
1996	1112.69	969.60	118.03	25.06	14.69	87.48	15.86
1997	1003.41	834.65	48.33	120.43	6.99	34.48	6.86
1998	1015.15	884.91	70.29	59.95	7.66	53.67	8.96
1999	715.80	673.35	21.73	20.72	1.55	16.55	3.63
2000	929.08	765.87	65.70	97.51	7.61	47.96	10.12
2001	1166.17	988.80	102.91	74.46	11.99	79.88	11.04
2002	958.23	895.88	57.03	5.32	4.25	43.05	9.73
2003	1101.16	963.84	100.81	36.51	14.61	75.21	10.99
Average	1006.31	878.16	79.37	48.78	8.71	59.64	11.02

Where, P is Precipitation, Q is total runoff,  $\Delta S$  is change in Storage, ETR is Evapotranspiration, Q<sub>DIR</sub> is Direct flow, Q<sub>INT</sub> Inter flow, Q<sub>BASE</sub> is Base flow.

**Table 13** | Annual water balance (in mm) for Bilate watershed area for the validation period (2007–2015) for LULC\_1989

Year	P	ETR	Q	$\Delta S$	Q <sub>DIR</sub>	Q <sub>INT</sub>	Q <sub>BAS</sub>
2007	1133.59	1010.06	58.94	64.59	6.24	39.05	13.65
2008	1025.70	913.95	43.47	68.28	3.96	31.09	8.43
2009	910.39	813.42	36.00	60.97	2.37	25.22	8.41
2010	1197.51	1032.93	144.68	19.90	19.75	110.90	14.04
2011	945.56	877.70	42.08	25.78	3.36	29.56	9.17
2012	859.41	741.31	41.98	76.12	2.00	29.34	10.63
2013	1180.71	1022.47	112.40	45.84	11.02	80.76	20.62
2014	1105.60	904.38	153.19	48.03	15.86	115.63	21.69
2015	899.50	772.89	41.41	85.20	2.73	30.84	7.84
Average	1028.66	898.79	74.91	54.97	7.48	54.71	12.72

Where, P is Precipitation, Q is total runoff,  $\Delta S$  is change in Storage, ETR is Evapotranspiration, Q<sub>DIR</sub> is Direct flow, Q<sub>INT</sub> Inter flow, Q<sub>BASE</sub> is Base flow.

The annual simulation of hydrological processes was analyzed for LULC\_1989, LULC\_2002, and LULC\_2015 data. The result indicated that there was a change in total simulation flow, evapotranspiration, surface runoff, base flow and inters flow in each land use/land cover data (Table 12). In the study year intervals (1989–2015), change in total simulated flow increased by 77.83%, and direct runoff, interflow, and base flow increased by 80.23%, 75.69%, and 87.79% respectively. Hence, evapotranspiration decreased by 6% throughout the study time.

Hydrological cycling in a watershed can be characterized and quantified by a water balance, which is the computation of all water fluxes at the boundaries of the system under consideration. It is an itemized statement of all

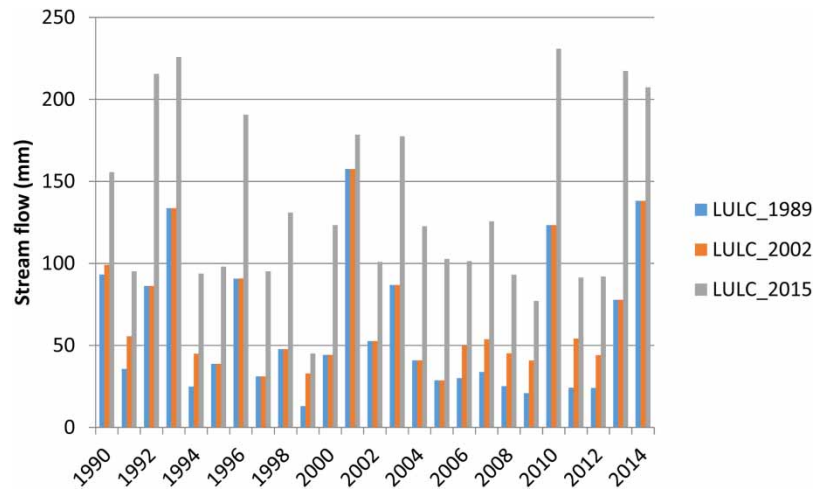


**Figure 11** | The change in mean annual stream flows due to the land use/land cover change.

gains, losses, and changes of water storage within a specified elementary volume of soil. From this study, rainfall was considered the gain, where evapotranspiration, total simulated flow (runoff, interflow, and base flow) were considered as the losses (Table 14).

**Table 14** | Hydrological process from annual simulations of 1989, 2002 and 2015 land use land covers

Hydrological processes	LULC_1989	LULC_2002	LULC_2015
Evapotranspiration(ETR),mm	890.84	887.84	837.58
Total simulated flow(Q), mm	74.898	86.08	133.34
Surface runoff( $Q_{DIR}$ ), mm	7.844	9.02	14.13
Inter flow( $Q_{INT}$ ), mm	55.50	59.00	97.51
Base flow( $Q_{BAS}$ ), mm	11.55	12.50	21.69

#### 4. CONCLUSION

In this study, we analyzed the impact of land use/land cover change on the water balance of the Bilate watershed. As part of our analysis, we considered six dominant land use/land covers including mixed forest, cultivation/agricultural land, barren land, grassland/pasture, range and shrub land, and settlement on the Bilate watershed for LULC\_1989, LULC\_2002, and LULC\_2015. Like many before us, we found ArcGIS to be a very important tool for the preparation of input data for analyses and the WaSiM model to be important for considering land use land cover data, soil, and DEM data.

The advancement of computational power and the availability of spatial and temporal data have made hydrological models attractive tools to examine and analyze the characteristics of watersheds and how the hydrological process of the catchment functions under varying land-use dynamics. Particularly in this study, hydrological modeling is a useful tool for investigating interactions among the watershed components and hydrologic response analysis to LULCC at various spatial and temporal scales.

The simulated water balance for the Bilate watershed using the WaSiM-ETH showed the interflow component of the water balance takes a higher fraction of simulated discharge and also surface runoff and total simulation flow increased through the study period. Additionally, the ETR, ETP, and soil storage capacity decreased throughout the study periods. Overall, the hydrological model describes changes in the water balance from 1989 to 2015, which indicate that the change in total simulated flow increased by 77.83%, and direct runoff, interflow, and base flow increased by 80.23%, 75.69%, and 87.79% respectively. Additionally, evapotranspiration decreased by 6% throughout the study time.

The future sustainable land and water resources in the Bilate watershed depend on the spatial planning of land use to optimize environmental benefits. Factors that must be considered include managing surface runoff control,

erosion protection, flood protection, and water availability. Finally, educating the community on the effect of the unplanned land-use practices on the environment, natural resources, and ecosystem are of paramount importance for the future sustainability of the watershed.

## ACKNOWLEDGEMENTS

Special thanks are due to the Ethiopian National Meteorological Agency and Ethiopian Ministry of Water, Irrigation, and Electricity for providing us with the meteorological and hydrological data.

## DISCLOSURE STATEMENT

The authors declare no conflict of interest.

## DATA AVAILABILITY STATEMENT

All relevant data are included in the paper or its Supplementary Information.

## REFERENCES

- Amiri, S. 2011 On the application of bootstrap, coefficient of variation and contingency table, information theory and ranked set sampling. Dissertation, Uppsala University, Uppsala, Sweden.
- Asmamaw, L. B., Mohammed, A. A. & Lulseged, T. D. 2012 [Land use/cover dynamics and their effects in the Gerado catchment, northeastern Ethiopia](#). *International Journal of Environmental Studies* **68**, 883–900.
- Bahati, H. K., Ogenrwoth, A. & Sempewo, J. I. 2021 [Quantifying the potential impacts of land-use and climate change on hydropower reliability of Muzizi hydropower plant, Uganda](#). *Journal of Water and Climate Change* **273**, 12–22.
- Brath, A., Montanari, A. & Moretti, G. 2006 [Assessing the effect on flood frequency of land use change via hydrological simulation \(with uncertainty\)](#). *Journal of Hydrology* **324**, 141–153.
- Brincker, R., Zhang, L. & Andersen, P. 2001 [Modal identification of output-only systems using frequency domain decomposition](#). *Smart Materials and Structures* **10** (3), 441.
- CSA (Central Statistical Agency) 2013 *Summary and Statistical Report of the 2013 Population and Housing Census: Population Size by Age and Sex*. Federal Democratic Republic of Ethiopia Population Census Commission, Addis Ababa.
- DeFries, R. & Eshleman, K. 2004 [Land-use change and hydrologic processes: a major focus for the future](#). *Hydrological Processes* **18**, 2183–2186.
- Degelo, S. 2007 *Analysis of Biomass Degradation as an Indicator of Environmental Challenge Bilate Watershed Using GIS Techniques*. Addis Ababa University, Addis Ababa, Ethiopia.
- Deng, Z., Zhang, X., Li, D. & Pan, G. 2015 [Simulation of land use/land cover change and its effects on the hydrological characteristics of the upper reaches of the Hanjiang Basin](#). *Environmental Earth Sciences* **73**(3), 1119–1132.
- Easton, Z., Fuka, D., White, E., Collick, A., BirukAsharge, B., McCartney, M., Awulachew, S., Ahmed, A. & Steenhuis, T. 2010. [A multi basin SWAT model analysis of runoff and sedimentation in the Blue Nile, Ethiopia](#). *Hydrology and Earth System Sciences Discussions* **7**, 3837–3878.
- Farmer-Bowers, Q., Crosthwaite, J., Callaghan, J., Hollier, C. & Straker, A. 2006 Drivers of land use change, Final Report: Matching opportunities to motivations, ESAI project 05116. *Department of Sustainability and Environment and Primary Industries*, Royal Melbourne Institute of Technology, Australia.
- Fox, A. L., Eisenhauer, D. E. & Dosskey, M. G. 2005 Modeling Water and Sediment Trapping by Vegetated Filters Using VFSSMOD: Comparing Methods for Estimating Infiltration Parameters. In: *ASAE Annual International Meeting, 17-20 July, Tampa, Florida*. Society for Engineering in Agricultural, Food and Biological Systems, St Joseph, MI.
- Getahun, G. 2017 *Local Adaptation Practices in Response to Climate Change in the Bilate River Basin, Southern Ethiopia*. The University of South Africa.
- Green, W. H. & Ampt, G. A. 1911 Studies of soil physics, part I – the flow of air and water through soils. *J. Ag. Sci.* **4**, 11–24.
- Guo, H., Hu, Q. & Jiang, T. 2008 [Annual and seasonal streamflow responses to climate and land-cover changes in the Poyang Lake basin, China](#). *Journal of Hydrology* **355**, 106–122.
- Gwate, O., Woyessa, Y. E. & Wiberg, D. 2015 [Dynamics of land cover and impact on streamflow in the Modder River Basin of South Africa: case study of a quaternary catchment](#). *International Journal of Environmental Protection and Policy* **3**, 31–38.
- Hagos, M. K. 2014 Analysing the effect of land cover change on catchment discharge. Tigray Agricultural Research Institute, Tigray, Ethiopia.
- Hörmann, G., Horn, A. & Fohrer, N. 2005 [The evaluation of land-use options in mesoscale catchments: Prospects and limitations of eco-hydrological models](#). *Ecological Modelling* **187**, 3–14.
- Huisman, J., Breuer, L., Bormann, H., Bronstert, A., Croke, B., Frede, H.-G., Gräff, T., Hubrechts, L., Jakeman, A. & Kite, G. 2009 [Assessing the impact of land use change on hydrology by ensemble modeling \(LUCHEM\) III: Scenario analysis](#). *Advances in Water Resources* **32**, 159–170.

- Kaiser, M. 2014 Process based hydrological modeling of the Imnavait basin (Alaska). MSc Thesis, University of Alaska Fairbanks, Fairbanks, Alaska.
- Kebede, A., Diekkrüger, B. & Moges, S. A. 2013 *Downscaling Climate Model Outputs for Estimating the Impact of Climate Change on Water Availability Over the Baro-Akobo River Basin, Ethiopia*. The University of Bonn, Bonn, Germany.
- Lambin, E. F., Geist, H. J. & Lepers, E. 2003 *Dynamics of land use and land cover change in tropical regions*. *Annu. Rev. Environment. Resource* **28**, 205–241.
- Mengistu, K. 2009 *Watershed Hydrological Responses to Changes in Land Use and Land Cover, and Management Practices at Hare Watershed, Ethiopia*.
- Nejad Hashemi, A., Wardynski, B. & Munoz, J. 2011 Evaluating the impacts of land-use changes on hydrologic responses in the agricultural regions of Michigan and Wisconsin. *Hydrology & Earth System Sciences Discussions* **8**, 3421–3468.
- PHE, Ethiopia Consortium 2011 *Proceeding of the National Workshop in Integrated Watershed Management On Gibe-Omo Basin*. Jimma University, Jimma, Ethiopia.
- Reichardt, K., Angelocci, L. R., Bacchi, O. O. S. & Pilotto, J. E. 1995 *Daily rainfall variability at a local scale (1,000 ha), in Piracicaba, SP, Brazil, and its implications on soil water recharge*. *Sci. Agric.* **52**, 43–49.
- Rutebuka, J., De Taeye, S., Kagabo, D. & Verdoodt, A. 2020 *Calibration and validation of rainfall erosivity estimators for application in Rwanda*. *Catena* **190**(1–3):104538.
- Schulla, J. & Jasper, K. 2012 *Model Description WASIM-ETH Manual*. Last updated: November 2012.
- Tubiello, F. N. & van der Velde, M. 2007 Land and water use options for climate change adaptation and mitigation in agriculture. UN Food and Agriculture Organization, New York, NY.
- Tufa, A. Y. & Srinivasarao, G. V. R. 2014 *Watershed Hydrological Response to U.S. Army Corps of Engineers (2001)*. Hydrologic Modeling System HEC-HMS University of Western Ontario.
- Wagesho, N. 2014 *Catchment Dynamics and its Impact on Runoff Generation: Coupling Watershed Modeling and Statistical Analysis to Detect Catchment Responses*. Arba Minch University, Arba Minch, Ethiopia.
- Wakjira, T. 2016 *Effects of Land use Land Cover Change on Hydrological Processes Gilgel Gibe, Omo Gibe Basin, Ethiopia*. The University of Rostock.
- Wösten, J. H. M., Lilly, A., Nemes, A. & Le Bas, C. 1999 Development and use of a database of hydraulic properties of European soils. Elsevier, New York, NY.

First received 11 January 2021; accepted in revised form 17 June 2021. Available online 7 July 2021